JOURNAL OF BACTERIOLOGY, Nov. 1998, p. 5529–5539 Vol. 180, No. 21
0021-9193/98/$04.00+0

Oxygen-Insensitive Nitroreductases: Analysis of the Roles of *nfsA* and *nfsB* in Development of Resistance to 5-Nitrofuran Derivatives in *Escherichia coli*

J. WHITEWAY, P. KOZIARZ, J. VEALL, N. SANDHU, P. KUMAR, B. HOECHER, AND I. B. LAMBERT*

Biology Department, Carleton University, Ottawa, Ontario, Canada K1S 5B6

Received 9 April 1998/Accepted 17 August 1998

Nitroheterocyclic and nitroaromatic compounds constitute an enormous range of chemicals whose potent biological activity has significant human health and environmental implications. The biological activity of nitro-substituted compounds is derived from reductive metabolism of the nitro moiety, a process catalyzed by a variety of nitroreductase activities. Resistance of bacteria to nitro-substituted compounds is believed to result primarily from mutations in genes encoding oxygen-insensitive nitroreductases. We have characterized the *nfsA* and *nfsB* genes of a large number of nitrofuran-resistant mutants of *Escherichia coli* and have correlated mutation with cell extract nitroreductase activity. Our studies demonstrate that first-step resistance to furazolidone or nitrofurazone results from an *nfsA* mutation, while the increased resistance associated with second-step mutants is a consequence of an *nfsB* mutation. Inferences made from mutation about the structure-function relationships of NfsA and NfsB are discussed, especially with regard to the identification of flavin mononucleotide binding sites. We show that expression of plasmid-carried *nfsA* and *nfsB* genes in resistant mutants restores sensitivity to nitrofurans. Among the 20 first-step and 53 second-step mutants isolated in this study, 65 and 49%, respectively, contained insertion sequence elements in *nfsA* and *nfsB*. IS*1* integrated in both genes, while IS*30* and IS*186* were found only in *nfsA* and IS*2* and IS*5* were observed only in *nfsB*. Insertion hot spots for IS*30* and IS*186* are indicated in *nfsA*, and a hot spot for IS*5* insertion is evident in *nfsB*. We discuss potential regional and sequence-specific determinants for insertion sequence element integration in *nfsA* and *nfsB*.

Nitroheterocyclic and nitroaromatic compounds constitute an enormous range of chemicals that are characterized by the presence of one or more nitro groups on a heterocyclic or aromatic nucleus. For many years nitro-substituted compounds have been used in manufacturing processes (23, 67) and as antimicrobial agents (49, 70). More recently, nitropolyaromatic compounds have been identified as by-products of a variety of combustion processes (20, 21, 52, 62, 63, 71). Human health concern in regard to all of these compounds has resulted from the identification of several nitro derivatives as potent bacterial mutagens, mammalian cell mutagens and clastogens, and rodent carcinogens (4, 37, 71).

The biological activity of nitro-substituted compounds is derived from reductive metabolism of the parent compound's nitro moiety, a process catalyzed by a variety of nitroreductase activities (12, 24, 49, 59). Metabolism of nitroaromatic compounds proceeding through two-electron reduction of the nitro moiety yields nitroso and hydroxylamine intermediates and an amino-substituted product. Metabolism of 5-nitrofuran compounds produces an open-chain nitrile isomer in addition to the aminofuran derivative (49). The end products of metabolism are biologically inactive; the biological activities of these chemicals are conferred by the reactivities of short-lived intermediates with protein and DNA. Nitroreduction proceeding through single-electron increments yields an additional product, the nitro-anion free radical, at the first step. Reoxidation of this radical intermediate in the presence of oxygen accounts for the oxygen sensitivity of some biological nitroreductases (43, 49, 59).

In *Escherichia coli* two classes of nitroreductase can be distinguished based on their sensitivities to oxygen: oxygen-insensitive (type I) nitroreductases and oxygen-sensitive (type II) nitroreductases (2, 22, 46, 59). The *nfsA* gene (*mdaA* [8]), located at 19.2 min on the *E. coli* chromosome, has recently been cloned (79) and encodes the protein previously described as nitroreductase IA (14). NfsA is a flavin mononucleotide (FMN)-containing protein with a monomeric molecular mass of 26.8 kDa that uses NADPH as an electron donor (14, 79). The nitroreductase gene *nfsB* (*nfnB* [51]), located at 13 min on the *E. coli* chromosome (8), appears to encode the minor nitroreductase component previously referred to as IB_1 (14). The NfsB protein is an FMN-containing flavoprotein with a monomeric molecular mass of approximately 24 kDa; NfsB can use either NADH or NADPH as a source of reducing equivalents (14, 51). The genes encoding type I nitroreductase IB_2 (14) and type II nitroreductases have not yet been identified.

Bacterial resistance to antimicrobial nitroheterocyclic agents occurs in a stepwise manner. Early biochemical studies of nitroreductase mutants (14, 45, 48) suggested that increased resistance is associated with the sequential mutagenic inactivation of multiple nitroreductases (14, 48, 64). Although *E. coli* genes encoding the NfsA and NfsB nitroreductases have now been identified, the direct link between mutation in these genes and the development of bacterial resistance has yet to be established. To address this point, we have returned to several nitrofurazone-resistant mutants that were well characterized in

* Corresponding author. Mailing address: Biology Department, Carleton University, 1125 Colonel By Dr., Ottawa, Ontario, Canada K1S 5B6. Phone: (613) 520-2600, ext. 2755. Fax: (613) 520-4497. E-mail: ilambert@ccs.carleton.ca.

earlier studies (14, 48) and have isolated a large number of additional first- and second-step furazolidone-resistant mutants. We have analyzed the cross-resistance of the mutants, determined cellular nitroreductase activities, and characterized the DNA sequence alterations in the *nfsA* and *nfsB* genes.

MATERIALS AND METHODS

Bacterial strains, plasmids, and growth conditions. *E. coli* K-12 strains AB1157, NFR402, NFR502, and SIL41 were provided by D. Bryant, McMaster University, Hamilton, Canada. AB1157 (F$^-$ *thr-1 leu-6 thi-1 supE44 lacY1 galK2 ara-14 xyl-5 mtl-1 proA2 his-4 argE3 str-31 tsx-33* λ^- *sup-37*) (3) is the parent strain of the putative nitroreductase mutants NFR402, and NFR502 (48). Strain SIL41 was derived from a cross between AB1157 and an HfrH strain lacking NfsA and NfsB activities (14). DH5α [*supE44 lacU169* (ϕ80*lacZ*ΔM15) *hsdR17 recA1 endA1 gyrA96 thi-1 relA1*] is a standard laboratory strain used for most plasmid manipulations. INVαF′ [F′ *endA1 recA1 hsdR17* (r_K^- m_K^+) *supE44 thi-1 gyrA96 relA1* ϕ80*lacZ*ΔM15 Δ(*lacZYA-argF*)*U169* λ^-] was included in the Original TA Cloning Kit. The vectors used in this study were pUC118 (76), pKK232-8 from Pharmacia Biotech Inc. (11), and pCR 2.1 from the Original TA Cloning Kit. Bacterial strains were routinely grown at 37°C in Luria-Bertani (LB) medium or on LBA (LB medium with 1.5% agar), obtained as a premixed powder from Canadian Life Technologies Inc. (Burlington, Ontario, Canada). When appropriate, the medium was supplemented with antibiotics at the following concentrations: 100 μg of ampicillin per ml, 30 μg of chloramphenicol per ml, and 50 μg of kanamycin per ml. Nitrofurazone (5-nitro-2-furaldehyde semicarbazone) and furazolidone were kind gifts from D. Bryant, McMaster University; stock solutions were prepared in dimethyl sulfoxide.

Isolation of furazolidone-resistant strains. Furazolidone-resistant mutants were obtained as described previously but with furazolidone instead of nitrofurazone (48). Briefly, furazolidone gradient plates were prepared as previously described (68); 24 h was allowed for diffusion of the drug prior to plating. Multiple cultures of AB1157 were grown to exponential growth phase and spread on the furazolidone gradient plates (0 to 1.25 μg/ml), which were incubated overnight. Several colonies representing independent first-step mutants, were selected, subcultured, and grown on gradient plates containing higher concentrations of the drug (0 to 2.5 or 0 to 4 μg/ml). Isolated colonies on these plates represented second-step mutants.

Determination of nitrofurazone sensitivity. Overnight cultures of each mutant strain were streaked with an absorbent applicator onto a gradient plate containing 0 to 50 μg of nitrofurazone per ml. This provided a standard measure of resistance and allowed the new mutants to be compared with previously isolated strains (48). Absolute concentrations of nitrofurazone to which strains were tolerant were determined as described by McCalla's group (48): 10 μl of overnight cultures was inoculated in a grid pattern onto plates containing 5 to 45 μg of nitrofurazone per ml.

Preparation of cell extracts. Overnight cultures (6 ml) were harvested by centrifugation. The cells were washed and resuspended in 0.25 ml of Tris-HCl buffer (pH 7.0). The suspensions were chilled on ice, sonicated with a Kontes Micro-Ultrasonic cell disrupter, and centrifuged at 14,000 × *g* for 30 min at 4°C. The protein concentration was determined as described for the Bio-Rad (Richmond, Calif.) protein assay with a bovine serum albumin standard curve.

Nitroreductase assay. Nitroreductase activity was measured as nitrofurazone reductase. The reduction of nitrofurazone was determined by a decrease in the absorbance of nitrofurazone at 400 nm (molar extinction coefficient, 12,960 M^{-1} cm^{-1} [79]) at 22°C. The reaction mixture (1 ml) contained 50 mM Tris-HCl (pH 7.0), 0.1 mM nitrofurazone, and 0.1 mM NADPH.

Manipulation of DNA. Genomic DNA was isolated as described previously (61); DNA was collected by centrifugation (12,000 × *g*). Plasmid DNA was isolated by the boiling miniprep method described previously (36). If further purification was necessary, it was accomplished by using a GeneClean kit (Bio 101, Inc.). Standard procedures were used for molecular cloning.

Amplification of the *nfsA* and *nfsB* genes. Amplification of the *nfsA* (Fig. 1) and *nfsB* (Fig. 2) fragments from genomic DNA was accomplished by PCR with the Expand High Fidelity PCR System (Boehringer Mannheim Canada). Prior to amplification of *nfsA*, genomic DNA was denatured with 0.2 N NaOH. Prior to amplification of *nfsB*, genomic DNA was digested with *Hin*dIII (New England Biolabs). Reaction mixtures (100 μl) included the Expand High Fidelity buffer with 15 mM $MgCl_2$, 0.2 mM each deoxynucleoside triphosphate, 300 nM appropriate primers (Fig. 1 and 2), 1.7 U of Expand High Fidelity enzyme mix, and 20 to 750 ng of template DNA. Amplification was performed through 30 repetitions of a cycle of denaturation for 15 s at 94°C, annealing for 30 s at 55°C, and elongation for 1 min at 72°C, with the addition of a 4-min preincubation at 94°C and a 7-min postincubation at 72°C. Prior to further analysis, the products were purified by using a High Pure PCR Product Purification Kit (Boehringer Mannheim Canada). Amplification product and restriction endonuclease analyses were done by agarose gel electrophoresis (1%) in the presence of ethidium bromide.

Cloning of *nfsA* and *nfsB*. Cloning of amplified *nfsA* and *nfsB* into pCR 2.1 was carried out according to the Original TA Cloning Kit instructions with the following changes. The Expand High Fidelity PCR System was used to amplify *nfsA* from AB1157, followed by a 10-min incubation at 72°C with 1 U of *Taq* polymerase (Canadian Life Technologies Inc.) to add a 3′ A overhang. Successful clones, pTAA and pTAB, and sequence fidelity were verified by sequencing with universal primers for pUC vectors as well as with specific internal primers for *nfsA* and *nfsB*. The *nfsB* PCR fragment was inserted into the *Eco*RI and *Bam*HI sites of pUC118 to create pJAB. The primers used for amplification of the 850-bp *nfsB* fragment contained these 5′ restriction endonuclease recognition sites (Fig. 2) to facilitate cloning. pJAC was constructed by subcloning the 469-bp *Eco*RI (filled)-*Bgl*II fragment of pJAB into the *Sma*I and *Bam*HI sites of pKK232-8. The 3′ termini of *Eco*RI were filled in by adding 2 μl each of dATP and dTTP (1 mM stocks) and 2 U of Klenow polymerase to the pJAB *Eco*RI digest.

Sequencing of clones and PCR products. Sequencing of the *nfsA* and *nfsB* PCR products from each mutant was achieved by using the Sequenase version 2.0 T7 DNA Sequencing Kit and α-^{35}S-dATP (Amersham Canada Ltd.). The double-stranded template was denatured by boiling with 15 pmol of primer and quickly chilled on ice. The reaction products were analyzed on an 8% acrylamide-bisacrylamide gel.

Insertion sequence (IS) elements in *nfsA* and *nfsB* were identified by DNA sequencing of the gene or IS element endpoints followed by a nonredundant similarity search of sequence databases and the *E. coli* databank (Nara Institute of Science and Technology, Nara, Japan) with BLASTX (1).

Nitrofurazone sensitivity assay. Overnight cultures (100 μl) of each strain were added to 4 ml of LB top agar (LB medium solidified with 0.7% agar) to create a lawn of bacteria on which 10-μl amounts of nitrofurazone at various concentrations in dimethyl sulfoxide were applied in triplicate to paper disks arranged on the lawn. Overnight incubation at 37°C yielded cleared zones in the bacterial lawn, the diameters of which were measured.

CAT assay. The specific activity of chloramphenicol acetyltransferase (CAT) was determined by a previously described spectrophotometric assay (61). This method measures free 5-thio-2-nitrobenzoate at λ = 412 nm, which has a direct molar relationship to the acetylation of chloramphenicol in the presence of 5,5′-dithiobis-2-nitrobenzoic acid and acetyl coenzyme A (66).

Protein sequence analysis. A similarity search of protein sequence databases was conducted by using the BLAST server program (1) with default parameters. Protein alignments were performed by the ClustalV program (34) with default parameters.

RESULTS

Isolation of mutant strains. Putative nitroreductase mutants derived from AB1157 were identified based on their resistance to furazolidone after stepwise selection on gradient plates. Resistance to nitrofurazone as measured by growth on a gradient plate was used to standardize the level of nitrofuran resistance exhibited by our mutants and allow comparison to mutants selected in previous studies (14, 48). The first and second selection steps yielded mutants that were resistant to nitrofurazone concentrations of approximately 15 and 35 μg/ml, respectively. Resistance occurred incrementally; there were no instances in which a single selection step yielded a mutant that exhibited the resistance to the elevated concentrations of furazolidone that is characteristic of second-step mutants. Subsequent selection steps did yield third-step mutants which exhibited resistance to still-higher concentrations of furazolidone (>4 μg/ml). We have focused on the genetic analysis of first- and second-step mutants.

Genetic analysis. DNA sequence analysis was performed on the PCR-generated amplified products of *nfsA* and *nfsB* obtained from all of the furazolidone-resistant mutants isolated in this study, as well as from the nitrofurazone-resistant mutants NFR402, NFR502, and SIL41 obtained previously by other workers (48). Following sequence analysis, some mutants derived through a single experiment had identical mutations. To ensure that all mutations were of independent origin, only one identical mutant from each experiment was considered in our analysis. NFR402 is a first-step mutant with IS*186* integrated within the coding region of *nfsA* at position G^{388} (Fig. 1); NFR402 contains a wild-type *nfsB* gene. NFR502, a second-step mutant derived from NFR402, contains the identically integrated IS*186* in *nfsA*, as well as a missense mutation in *nfsB* at position C^{134} resulting in a Pro-to-Leu substitution at position 45 (Fig. 2). SIL41 was derived from a genetic cross be-

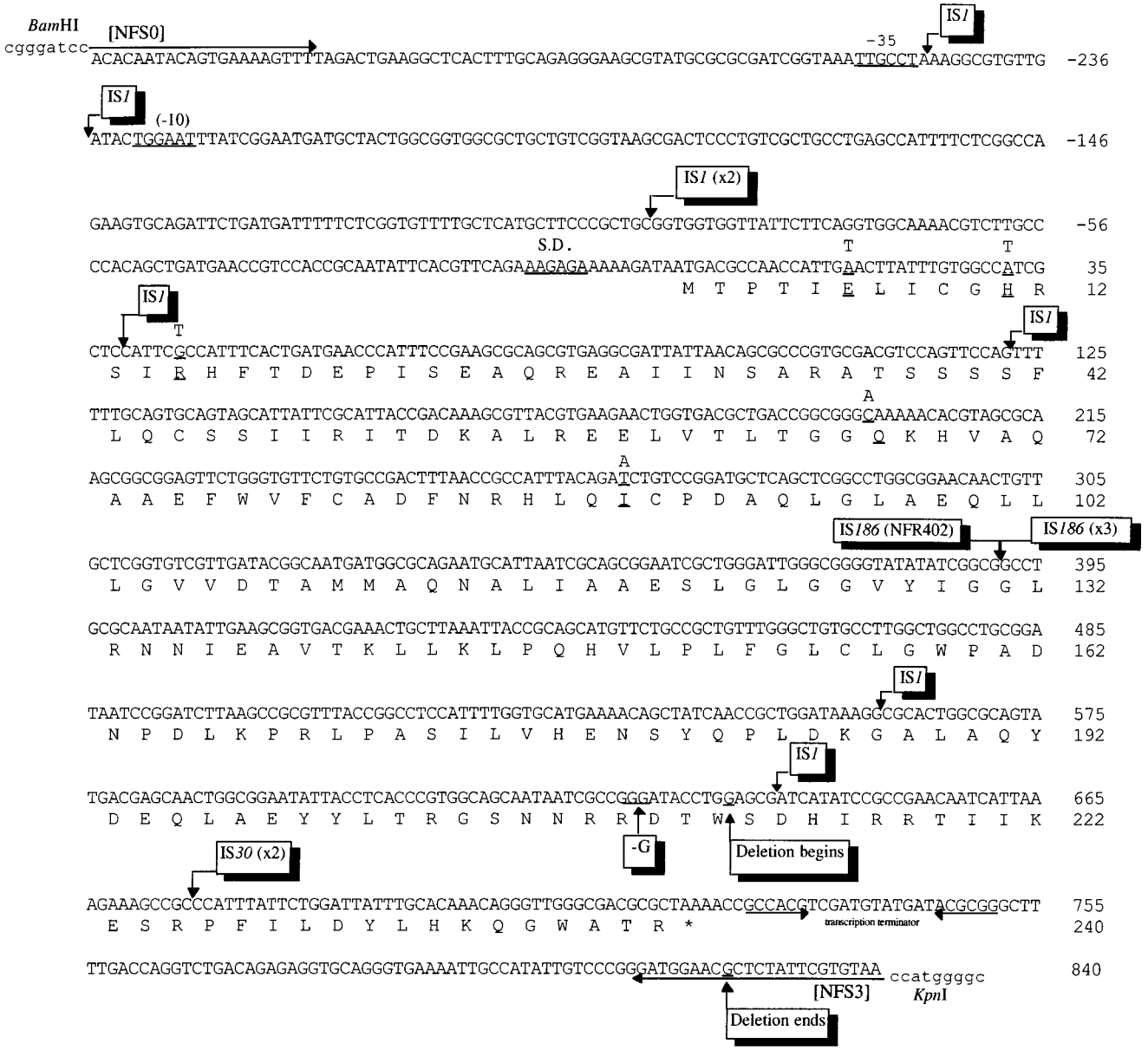

FIG. 1. Nucleotide sequence of the PCR-generated fragment containing the wild-type *nfsA* gene from *E. coli* AB1157, with putative −35 and −10 promoter elements, ribosomal binding site, and transcription terminator indicated. NFR402 refers to the mutants selected by McCalla and coworkers (47). Mutations for the 20 mutants characterized in this study are indicated. Altered bases and amino acids are underlined in the wild-type sequence, with substituted bases indicated above the sequence. IS elements are shown as boxes above the sequence, with arrows indicating the insertion point. Deletions and frameshifts are indicated below the sequence. PCR primers used for amplification of the gene are shown as horizontal arrows, and the lowercase letters indicate synthetic restriction endonuclease sites. S.D., Shine-Dalgarno sequence.

tween an Hfr *nfsA nfsB* double mutant and AB1157 and exhibits wild-type levels of resistance to nitrofurazone. However, SIL41 can be mutated to high (two-step) levels of nitrofuran resistance through a single mutational step. SIL41 has a wild-type *nfsA* gene and contains an amber mutation, Gln-142 (CAG) to amber (TAG), at position C^{424} in *nfsB* (Fig. 2).

All 20 of the first-step nitrofuran-resistant mutants isolated in this study contain a mutation in the *nfsA* gene (Table 1). No mutations in the *nfsB* gene were observed in any of the first-step mutants, while all but 4 of the 53 second-step mutants had a mutation in the *nfsB* gene (Table 1).

Among the first-step mutants selected in the current study, all have a single mutation affecting *nfsA*. All five base substitution mutations are located within the first third of the gene's coding region (Fig. 1). One mutant, JVR1, has a −1 frameshift resulting from a −G event at position $G^{626–628}$, thereby altering the remaining 31 amino acids and adding 15 more residues on the carboxyl terminus of the NfsA protein. One *nfsA* mutant, JVQ1, has a 177-base deletion, including the final 88 bases of the *nfsA* gene's coding region. The other 13 first-step mutants, comprising 65% of all the *nfsA* mutations, have IS elements integrated within and upstream of the coding region of *nfsA*. IS*1*, IS*30*, and IS*186* were identified in *nfsA*. Eight of the mutants contain IS*1*: four with integrations in the putative promoter region upstream of the coding sequence and two near each terminus of the gene. IS*30* integrated near the 5′ end

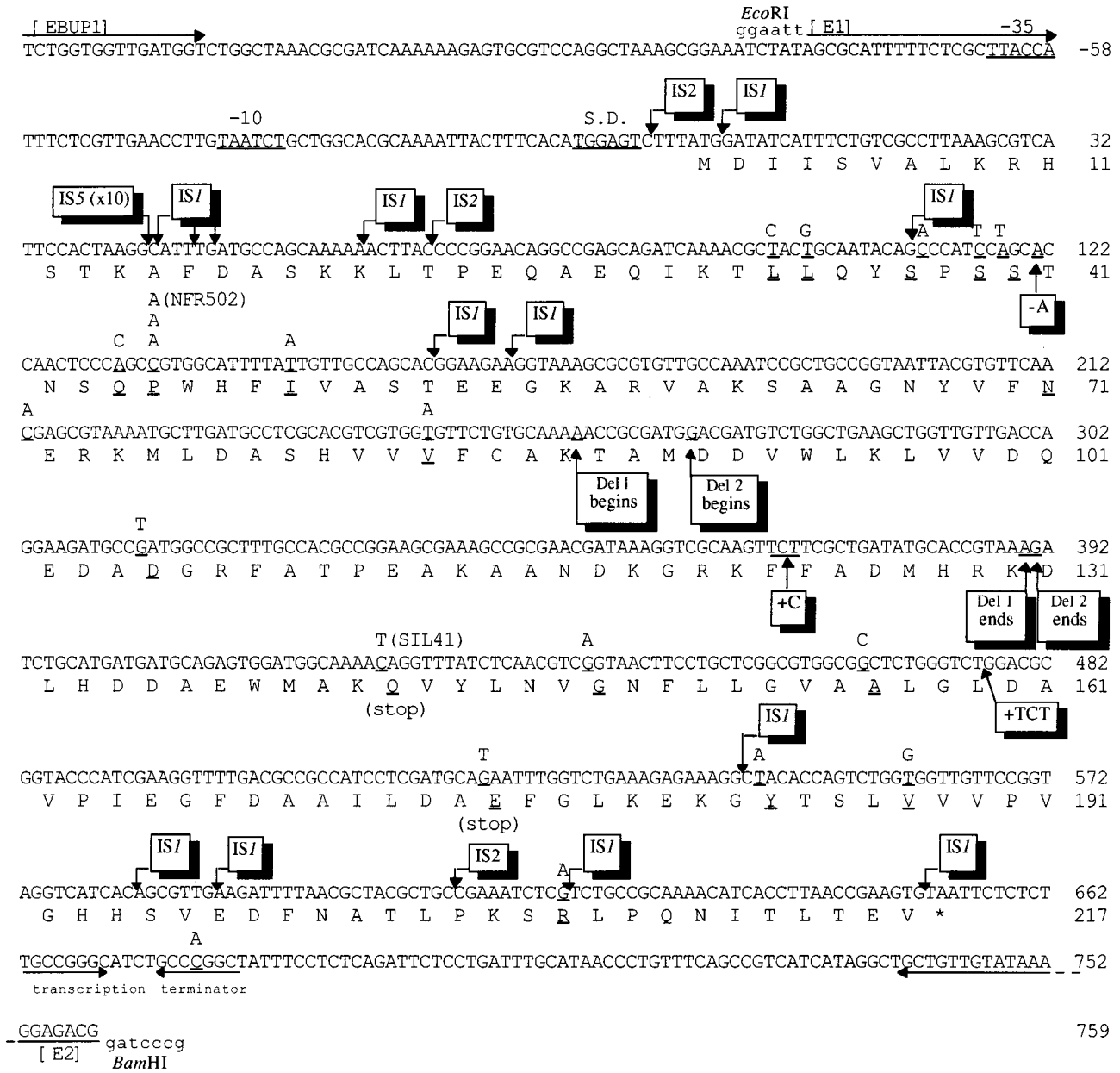

FIG. 2. Nucleotide sequence of the PCR-generated fragment containing the *nfsB* gene from *E. coli* AB1157 with putative −35 and −10 promoter elements, ribosomal binding site, and transcription terminator indicated. NFR502 and SIL41 refer to the mutants selected by McCalla and coworkers (14, 47). Mutations for the 53 mutants characterized in this study are indicated. Altered bases and amino acids are underlined in the wild-type sequence, with substituted bases indicated above the sequence. IS elements are shown as boxes above the sequence, with arrows indicating the insertion point. Deletions and frameshifts are indicated below the sequence. The horizontal arrows represent the PCR primers. Lowercase letters indicate the synthetic restriction endonuclease sites added to the PCR primers. S.D., Shine-Dalgarno sequence.

of *nfsA* in two mutants, both at position C^{675}. IS*186* is the only IS element that integrated near the middle of *nfsA*, and it is found in all three mutants at the identical position.

The second-step mutants isolated in this study were confirmed to have only the parental mutation in *nfsA*. Only single mutations were found in the *nfsB* genes of second-step mutants. Eighteen of the 53 second-step mutants have a base substitution in *nfsB*; 1 results in an ochre mutation, and 17 are missense mutations. Of the 17 missense mutations, 9 effected changes in a 17-amino-acid sequence, from Leu-33 to Ile-49, of the protein NfsB (Fig. 2). One mutant, JVZ2, has a three-base insert (TCT) at position T^{477} that results in the addition of a leucine residue between Leu-159 and Asp-160 (Fig. 2). The two mutants JVAE6 and JVI3 contain frameshift mutations in *nfsB* resulting from the insertion of a cytosine at position C^{369} and the deletion of A^{121}, events causing premature termination of translation after 2 and 53 amino acids, respectively. In two mutants, JVQ3 and JVR4, nearly identical deletions of approximately 80 bp are situated in the middle of the gene (Fig. 2). The most frequent type of mutation identified in the *nfsB* gene of the furazolidone-resistant mutants is IS element integration. Three IS elements, IS*1*, IS*2*, and IS*5*, account for 49% of the second-step mutants isolated in this study. With the one exception of IS*1* inserting near the Shine-Dalgarno sequence of

TABLE 1. Mutation distribution in *nfsA* and *nfsB* of nitrofuran-resistant mutants

Mutation	No. in:	
	nfsA of first-step mutants[a]	*nfsB* of second-step mutants[b]
Base substitutions		
Total	5	21
G · C→T · A	1	7
G · C→C · G	0	1
A · T→T · A	2	4
A · T→C · G	1	3
G · C→A · T	1	5[d]
A · T→G · C	0	1
Frameshifts and insertions		
Total	1	3
−G	1	0
−A	0	1
+C	0	1
+(TCT)	0	1
Deletions	1 (177 bp)	2 (~80bp)
Insertion elements		
Total	14	26
IS*1*	9[c]	13
IS*2*	0	3
IS*5*	0	10
IS*30*	2	0
IS*186*	3	0
None	0	3
Total no. of mutants	20 (21[c])	53 (55[d])

[a] The same mutations, and no others, are in *nfsA* of second-step mutants derived from first-step mutants.
[b] The *nfsB* gene of first-step mutants is wild type.
[c] The mutant NFR402 isolated by McCalla et al. (48) is included.
[d] The mutants NFR502 and SIL41 isolated by McCalla et al. (48) are included.

JVP3, all IS elements integrated within the coding region of *nfsB*. As in *nfsA*, IS elements demonstrated regional specificity for insertion in the regions proximate to either terminus of *nfsB*. This is particularly apparent in the first 165 bp of the gene's coding region, where IS element integration occurred in 19 mutants. IS*5* integrated at the identical sequence, after G^{43} (Fig. 2), in all 10 mutants with this element; IS*5* inserted in the identical orientation in each mutant except JVD2, in which it was reversed.

In four second-step mutants, no mutations were observed within the coding region of *nfsB*, although multiple sequencing reactions were carried out on both strands of the PCR products. Of these, one mutant, JVAE4, contained a transversion in the putative transcription terminator of *nfsB*. The resistance of the mutants JVA6, JVN3, and JVO2 to a concentration of nitrofurazone (35 μg/ml) consistent with a second-step mutant was confirmed. To ensure that there is not a mutation in or near the putative −35 region of *nfsB*, an upstream primer, EBUP1 (Fig. 2), was used to amplify and sequence this region. No mutations were found. We confirmed the presence of a functional promoter in the PCR-amplified product of *nfsB* by using the construct pJAC. pJAC contains the promoterless CAT gene of plasmid pKK232-8 directly downstream from the truncated fragment of the wild-type *nfsB*, containing the putative promoter region, so that any expression of CAT, and hence resistance to chloramphenicol, was due to the promoter activity of *nfsB*. Growth of transformants derived from pJAC on chloramphenicol medium confirmed the presence of a functional *nfsB* promoter in the PCR-amplified product. This construct enabled the measurement of promoter activity by determination of the specific activity of CAT (126 nmol min^{-1} mg^{-1}). The specific activity of CAT in the negative control containing only pKK232-8 was zero.

Nitroreductase activity. Nitroreductase activities in cell extracts of AB1157 (wild type), first-step mutants, and second-step mutants were spectrophotometrically measured as the reduction of nitrofurazone by using NADPH as a source of reducing equivalents. The average NADPH-dependent nitroreductase activities of AB1157, first-step mutants, and second-step mutants were 7,900, 290, and 5.5 nmol min^{-1} mg^{-1}, respectively (Table 2). Four second-step mutants have significantly greater nitroreductase activity than the average: JVA6, JVN3, and JVO2, the three second-step mutants that do not have a mutation in NfsB; and JVA5, which has a missense mutation in NfsB. Of particular interest is JVA6, which has nitroreductase activity (261 ± 50 nmol min^{-1} mg^{-1}) comparable to that of a first-step mutant. JVN3 has activity (41 ± 4.3 nmol min^{-1} mg^{-1}) that is about twice that of JVA5 and JVO2.

TABLE 2. Nitroreductase activity in cell extracts of AB1157 and first- and second-step nitrofuran-resistant mutants

Strain	Mutation	Nitroreductase activity[a] (nmol min^{-1} mg of $protein^{-1}$)
AB1157 (wild type)		7,900 ± 760
First-step mutants		
All		290 ± 80[b]
NfsA missense		
JVC1	Gln^{67}→Pro	441 ± 6
JVK1	Arg^{15}→Cys	233 ± 4
JVO1	Ile^{89}→Asn	284 ± 6
JVY1	His^{11}→Leu	253 ± 44
Second-step mutants		
All		5.5 ± 4.0[c]
NfsB missense		
JVA5	Ser^{40}→Cys	22 ± 1.9
JVB4	Asp^{71}→Lys	4.0 ± 0.3
JVE2	Ser^{39}→Cys	7.9 ± 0.1
JVE4	Gly^{148}→Ser	3.1 ± 0.5
JVG2	Asp^{105}→Tyr	10 ± 9.4
JVH2	Leu^{33}→Pro	4.1 ± 0.7
JVI2	Val^{83}→Asp	6.2 ± 7.0
JVL6	Val^{187}→Glu	8.9 ± 4.6
JVP2	Ser^{37}→Arg	9.4 ± 0.6
JVQ4	Pro^{45}→Gln	7.8 ± 6.5
JVR3	Gln^{44}→Pro	11 ± 2.1
JVY2	Arg^{207}→His	6.8 ± 5.0
JVAE5	Pro^{45}→Gln	2.1 ± 1.8
JVAG3	Tyr^{183}→Asp	5.7 ± 0.8
JVAG6	Leu^{34}→Arg	0.7 ± 0.8
No mutation in NfsB		
JVA6		261 ± 50
JVN3		41 ± 4.3
JVO2		19 ± 1.1
JVAE4	Transcription terminator	9.4 ± 4.2

[a] Averages and standard deviations from assays done at least twice.
[b] Average for all 20 first-step mutants.
[c] Average for all 50 second-step mutants for which a mutation has been characterized. The cultures of five second-step mutants were not viable after storage, and enzyme activity was not determined. Genetic characterization of these mutants had revealed the following mutations in *nfsB*: two missense (Ala^{156}→Pro and Ile^{49}→Asn), one stop (Glu^{175}→ochre) and two IS elements (IS1^{62} and IS5^{43}).

TABLE 3. Diameters of cleared zones in a lawn of each strain with and without vector-encoded NfsA (pTAA) and NfsB (pTAB) after the application of 5 mg of nitrofurazone per ml

Strain	Diam (mm)[a] for strain with:		
	Vector alone (pTA)	pTAA	pTAB
AB1157	18.4 (0.4)	20.6 (0.5)	20.9 (0.5)
JVQ1	15.5 (0.5)	18.8 (1.3)	18.9 (0.7)
JVQ2	12.5 (0.5)	20 (1)	18.8 (0.8)

[a] Results are means (standard deviations) calculated from five determinations.

The second-step mutant JVAE4, which has a mutation in the transcription terminator but not in the coding region of *nfsB*, has nitroreductase activity consistent with second-step mutants.

Restoration of nitrofuran sensitivity by cloned NfsA and NfsB proteins. The influence of plasmid-encoded NfsA and NfsB in vivo was evaluated for the wild-type *E. coli* strain AB1157, a first-step mutant containing a 177-bp deletion in *nfsA* (JVQ1), and a second-step mutant derived from JVQ1 with IS*5* integrated after position 43 in *nfsB* (JVQ2) by comparing the levels of nitrofurazone sensitivity of the strains transformed with pTAA (*nfsA*) or pTAB (*nfsB*) to that of the strains transformed with vector alone (pTA). Sensitivities were compared by measuring the diameters of cleared zones around a nitrofurazone-infused paper disk on a lawn of bacteria (Table 3). The greatest differences in sensitivity were noted for nitrofurazone concentrations between 5 and 10 mg/ml. Further increases in sensitivity were not observed at concentrations above 10 mg/ml, and concentrations of 1 mg/ml or lower did not yield cleared zones at all.

The cleared-zone diameters calculated from five determinations with each strain are indicated in Table 3. From this experiment, four observations were made. (i) AB1157, JVQ1, and JVQ2 had significantly different sensitivities to nitrofurazone; AB1157 demonstrated the greatest sensitivity, and JVQ2 had the least. The sensitivity correlates with nitroreductase levels in cell extracts (Table 2). (ii) Upon the introduction of either plasmid-encoded nitroreductase, an increase in sensitivity over that exhibited by the strain transformed with vector alone was observed. The increases in AB1157 were presumably due to the multiple copies of the plasmid-encoded gene. (iii) Between strains, no significant difference between the sensitivities conferred by the *nfsA*- and the *nfsB*-containing clones was apparent. While the percent increase in sensitivity was far greater in the mutants than in the wild type, the absolute sensitivities of the transformants, as indicated by the diameter of the cleared zone in the lawn, were similar to that of AB1157 transformants. This maximum diameter could represent a limit either for the chemical's diffusion or for cellular sensitivity to nitrofurazone. (iv) Transformation with either *nfsA* or *nfsB* increases sensitivity of all strains to the same level.

DISCUSSION

The genetic and biochemical characterizations in this study corroborate previous studies that suggested that NfsA and NfsB nitroreductase activities are necessary for the majority of nitrofuran biological activity under aerobic conditions (1, 14). Furthermore, by restoring nitrofuran sensitivity through the introduction of cloned *nfsA* and *nfsB* in AB1157 (wild type) and its nitroreductase-deficient derivatives (Table 3), we have shown that NfsA and NfsB are sufficient for maximal nitroreductase activity. Selection of *E. coli* K-12 nitrofuran-resistant strains on medium supplemented with furazolidone (this study), nitrofurazone (45, 48), or nitrofurantoin (10, 64) consistently yields two discrete steps of increased resistance. In this study we show through DNA sequence analysis of a large number of nitrofuran-resistant mutants that the observed pattern of two-step resistance is a consequence of an obligatory first-step event, mutation in *nfsA*, followed by mutational inactivation in *nfsB*. Each step of increased resistance correlates with a decrease in nitroreductase activity in cell extracts (with the exception of JVA6, which exhibits second-step resistance but a first-step level of nitroreductase activity). The observation that SIL41 (*nfsA*$^+$ *nfsB* [amber]) exhibits wild-type nitrofurazone resistance, despite having a reduction in oxygen-sensitive nitroreductase activity of approximately 25% (14), shows that inactivation of *nfsB* does not produce a resistance phenotype in the presence of a wild-type *nfsA* gene. However, in contrast to wild-type bacteria, SIL41 can attain a high (second-step) level of nitrofurazone resistance in a single step that presumably corresponds to inactivation of *nfsA*. Since the majority of aerobic nitroreductase activity is attributable to NfsA (Table 2), the simplest explanation for these results is that the loss of only the minor NfsB component from *nfsA*$^+$ strains is insufficient to reduce the total amount of nitroreductase activity to the extent that altered resistance will be conferred on the bacterium.

Of the mutants selected in this study, three second-step mutants did not have a mutation either in the coding region of *nfsB* or in the 100 bases upstream of the coding region, and one had a base substitution downstream of the coding region in the putative transcription terminator (Fig. 2). Confirmation that this *nfsB* fragment contained a functional promoter was achieved by demonstrating CAT activity in the plasmid pKK232-8, which contains a promoterless CAT gene, upon insertion of the putative promoter region of *nfsB*. We have also shown that NfsB is normally sufficient for biological activation of nitrofurans: sensitivity to nitrofurazone is increased upon the introduction of vector-encoded NfsB in both wild-type and mutant *E. coli* cells. In each of the three mutants resistance to elevated concentrations of nitrofurazone and furazolidone has been confirmed, eliminating the possibility of mutant reversion. Interestingly, each mutant has extract nitroreductase levels that are atypical of second-step mutants, with JVA6 exhibiting nitroreductase levels similar to those of first-step mutants and JVN3 and JFO2 exhibiting intermediate nitroreductase levels. This suggests that additional factors may modulate nitrofuran resistance. Possible explanations include (i) a nitroreductase enzyme distinct from NfsA or NfsB (for example, nitroreductase component IB_2, described by Bryant and coworkers [14]), (ii) a *trans*-acting factor with which interaction is essential for full nitroreductase activity; or (iii) a factor mediating transport of the nitrofuran into the cell. The last possibility seems particularly applicable to JVA6.

Beyond the initial two levels of resistance, nitrofurantoin- and furazolidone-isolated mutants appear to have nitrofuran tolerance properties not shared by nitrofurazone-resistant mutants. Third-step furazolidone-resistant mutants displayed inconsistent and nonuniform resistance when plated on nitrofurazone medium. Similar characteristics were observed in putative third- and fourth-step nitrofurantoin-resistant mutants (10), which did not display cross-resistance to nitrofurazone but instead were characterized by a second-step level of nitrofurazone resistance. It is possible that the principal mode of toxic action of the reactive metabolites derived from nitroreduction differs between nitrofuran derivatives. For example, nitrofurans have a variety of toxic actions, including genotoxicity, metabolic effects, effects on nucleotide pools, and for-

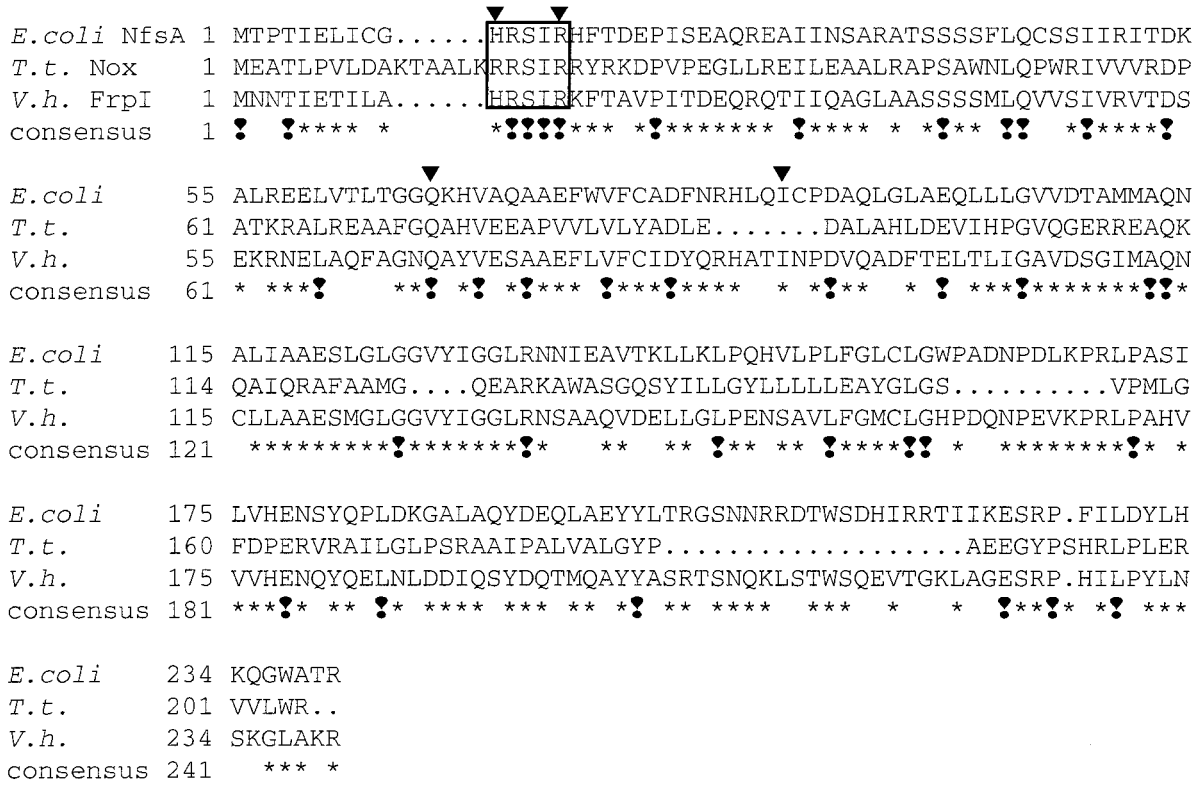

FIG. 3. ClustalV alignment of NfsA with *T. thermophilis* (*T.t.*) Nox and *V. harveyi* (*V.h.*) FrpI proteins. Exclamation points indicate completely conserved residues. Asterisks indicate residues, either identical or chemically similar, that are conserved between NfsA and one of the other proteins. The arrowheads above the sequences indicate residues altered in NfsA as a result of a mutation in *nfsA* of a furazolidone-resistant mutant. The five residues in the box comprise the putative FMN binding site (see text for details).

mation of active oxygen species (47, 73). Alternatively, the participation of other, as-yet-uncharacterized, nitroreductase activities may contribute to the reduction of a subset of nitrofuran derivatives (e.g., furazolidone and nitrofuranoin, but not nitrofurazone) in the absence of NfsA and NfsB activity. A third possibility is that the high levels of unreduced nitrofurazone in higher-order nitroreductase mutants may have an inhibitory effect on bacterial metabolism when mutants are plated on nitrofurazone medium (41).

The mutational distribution in the *nfsA* and *nfsB* genes of the nitrofuran-resistant mutants (Fig. 1 and 2) implicates particular residues as having functional significance in the NfsA and NfsB proteins. NfsA nitroreductase has 51 and 24% amino acid identity with NADH oxidoreductase (Frp) from *Vibrio harveyi* and NADH oxidase (Nox) from *Thermus thermophilus*, respectively (Fig. 3). The three-dimensional structures of both Frp (69) and Nox (33) have been determined experimentally, and the similarities between the two structures suggest that both Frp and Nox belong to the same group of flavoproteins. It is quite likely that NfsA constitutes another member of this group, since both Frp and Nox exist in the physiological state as homodimers, with gel exclusion chromatography data suggesting the same for NfsA (79). All three oxidoreductases use FMN as a cofactor (although Nox can also use flavin adenine dinucleotide [FAD]) and display kinetic profiles characteristic of a ping-pong bi-bi reaction mechanism (33, 69, 79). Particularly interesting is the conservation of the amino acid region corresponding to residues 11 to 15 of NfsA (Fig. 3) in the three flavoproteins, which has been shown to be involved in cofactor binding in both Frp and Nox. Two of four amino acid substitutions recovered from *nfsA* mutants characterized in this study are confined to this region (His-11 to Lys and Arg-15 to Cys); the change of a conserved residue, Gln-67, to His in another *nfsA* mutant could also be localized to the putative cofactor binding site, since glutamine residues in Frp and in Nox, corresponding to Gln-67 of NfsA, form two hydrogen bonds with the isoalloxazine ring of FMN (33, 69). These data suggest conservation of the basic cofactor binding site among the three flavoproteins.

NfsB has 85% amino acid sequence identity with homologous nitroreductases isolated from *Salmonella typhimurium* (78) and *Enterobacter cloacae* (13) and 32% identity with FRase I, the major flavin oxidoreductase of *Vibrio fischeri* (80, 81). The sequences of RdxA from *Helicobacter pylori* (29, 72), Nox from *T. thermophilus* (33), and a putative protein from *Bacillus subtilis* (5) also have some amino acid sequence identity with NfsB, particularly within a 14-residue stretch corresponding to Ser-37 to Val-50, near the amino terminus (Fig. 4). Although the overall similarity of these sequences is low, the identity between the proteins in this 14-residue region is high: it is 100% for the *E. coli*, *S. typhimurium*, and *E. cloacae* proteins, and the *V. fischeri*, *H. pylori*, *B. subtilis*, and *T. thermophilus* proteins have 78, 71, 57, and 50% identity, respectively, with the NfsB sequence. It is interesting that of the 17 *nfsB* mutants with missense mutations, 7 of the mutations (41%) are located in this region. The other 10 missense mutations also affected conserved residues: Arg-207 is conserved in all seven proteins, while the other amino acids altered by mutation in NfsB were conserved in at least four of the proteins. No consensus sequences for NAD(P)H or FMN binding have been

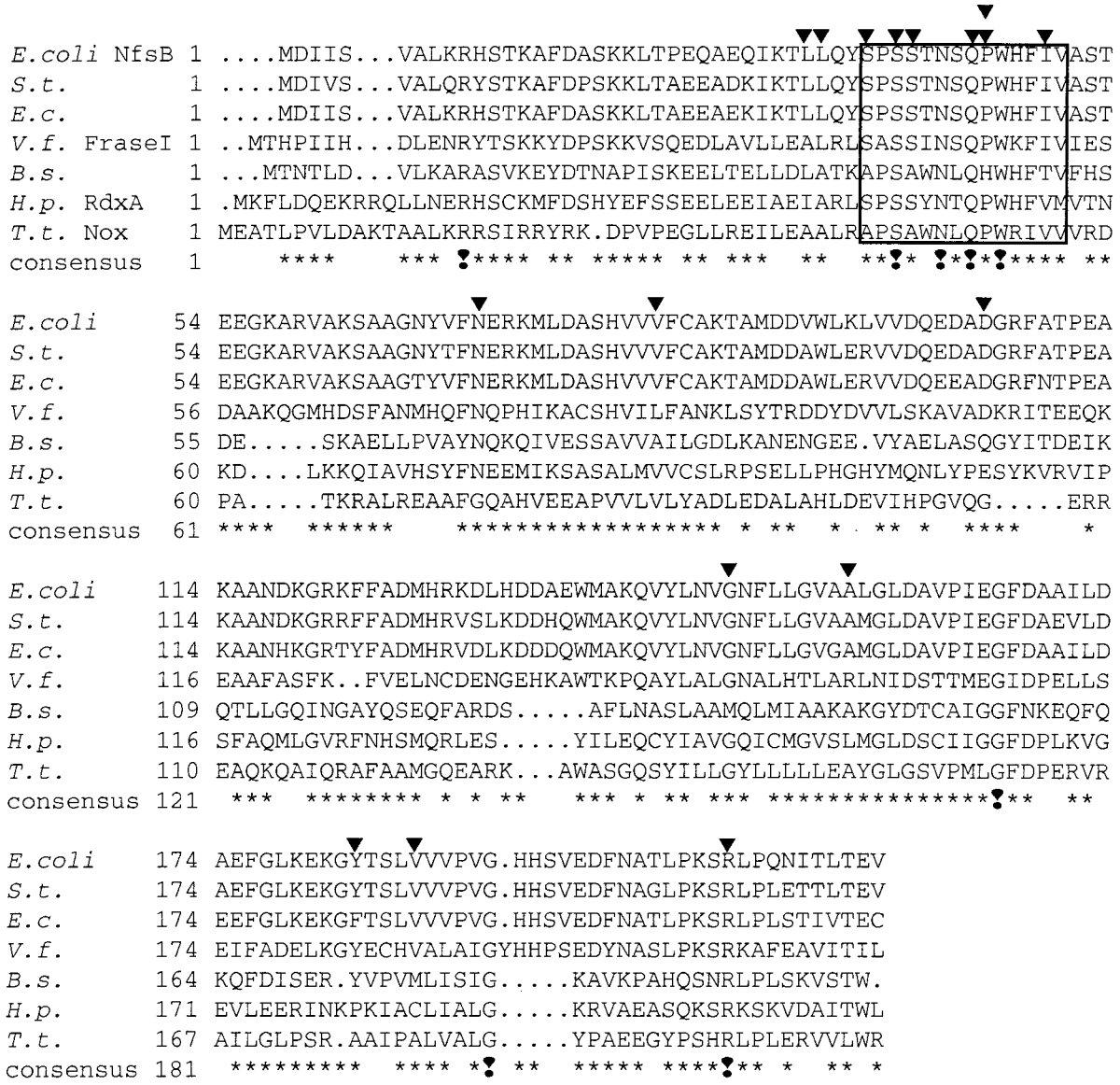

FIG. 4. ClustalV alignment of NfsB with the NfsB-like proteins from *S. typhimurium* (*S.t.*) and *E. cloacae* (*E.c.*), the major flavin reductase (FRase I) of *V. fischeri* (*V.f.*), the RdxA protein of *H. pylori* (*H.p.*), Nox of *T. thermophilus* (*T.t.*), and a hypothetical protein of *B. subtilis* (*B.s.*). Exclamation points indicate residues conserved in all seven proteins. Asterisks indicate residues, either identical or chemically similar, that are conserved in NfsB and at least three of the other proteins. The 14 residues indicated by the box constitute the most conserved region in the proteins and may include the FMN binding site (see text for details).

found in NfsB, either by searching the protein databases (PROSITE, PIR, and Swiss-Prot) with MotifFinder (28) or by comparisons with known FMN binding sites in other proteins (17, 35, 40, 42, 54–56, 58, 77). However, the amino acid sequence YSxSS (similar to the conserved sequence identified in this study at residues 36 to 40 of NfsB) was identified as part of the possible FAD-isoalloxazine ring binding region in two oxygenase enzymes of *Acinetobacter calcoaceticus* (55). The sulfite reductases of *E. coli* (17) and *S. typhimurium* (55) and the cytochrome P-450 oxidoreductases of pig and rat also contain a similar sequence, YSIAS, that aligns with the oxygenase enzymes and corresponds to FAD binding domains (55). Phe-124 appears to be spatially situated near the isoalloxazine ring of a bound flavin in NfsB, as manipulation of this residue can alter the affinity of NfsB for binding different flavins, and deletion of the residue substantially increases flavin reductase activity (80).

Among the 20 mutations isolated in the *nfsA* genes and the 50 mutations characterized for the *nfsB* genes of the furazolidone-resistant mutants isolated in this study, 13 (65%) and 26 (52%), respectively, were derived from the insertion of one of six IS elements (Table 1). Transposition is a rare event, occurring at frequencies of 10^{-7} to 10^{-5} per generation, with only 5 to 15% of all spontaneous mutations being attributed to IS elements (26). Although there is a high degree of variability in the copy number and presence of IS elements in *E. coli* strains (9), all IS element types identified in this study have been mapped to fixed locations on the chromosome of *E. coli* K-12 strains, as well as having additional strain-specific locations (6, 7, 9, 75). Clustering of particular IS families to certain chromosomal locations is believed to result from local hopping, a process in which local transposition events give rise to daughter IS elements inserted in close proximity (<10 kb) to the parent element (9, 18). The *nfsA* gene is located at 19.2 min on

the *E. coli* K-12 chromosome (8): no IS elements have previously been mapped within 10 kb (approximately 0.2 min) of *nfsA*. The *nfsB* gene is located at 13 min on the *E. coli* chromosome (8). IS*5*, at 13.1 min, is the only element identified in this study to be located near *nfsB* in the three mapped *E. coli* K-12 strains (6). Proximity of IS*5* to *nfsB* on the chromosome, in addition to the probable IS*5* hot spot in *nfsB* (discussed below), and the high transposition rate observed for IS*5* (53) could account for the large number of *nfsB* mutants (19%) containing IS*5* in this study.

There are two putative IS element hot spots in *nfsA* and one in *nfsB*. In *nfsA* a hot spot for IS*186* is indicated after G^{388}, as all three IS*186* mutants independently isolated in this study, as well as the previously isolated NFR402, had IS*186* inserted at this site (Fig. 1). The hot spot for IS*186* in *nfsA* is similar to the G+C-rich insertion sites observed in other studies (16, 39, 65), as it is directly downstream from two G_3 runs and one G_4 run. The target duplications, GC or GT, generated by IS*186* in the *nfsA* genes of mutants in this study and in NFR402 (48) were of identical length. In contrast, other studies noted that even at an identical integration site, the target duplications were of variable lengths (39, 65). Specific target sequences are often associated with the transposition of IS*30* (15, 26, 57). A putative hot spot for IS*30* insertion after C^{675} in *nfsA* is suggested by our data. The target site has similarities with the IS*30* hot spots observed in the prophage P1 and the R plasmid NR1-Basel (15): the sequence GCC immediately precedes the target duplication, and the sequence ANNNCCTTTNTTA, suggested to be involved in target site selection of IS*30* in P1 (15), is present, reversed and with one mismatch (A^{689} ACACGTT TATTA^{701}), immediately upstream of the IS*30* insertion site in *nfsA*. A hot spot for IS*5* after G^{43} is evident in *nfsB*: 10 independent mutants that contained IS*5* at the same site were isolated in this study. The target sequence for IS*5* in *nfsB*, AA GG^{43}, does not conform to the previously described IS*5* target site consensus sequence C(A/T)A(G/A) (25). However, of the 12 sequences within the coding region of *nfsB* that did match this consensus sequence, two, $CTAA^{41}$ and $TTTG^{49}$, flanked the insertion point of IS*5*.

IS element target site sequence specificity may sometimes be attributable to protein consensus sequences. In particular, *E. coli* integration host factor (IHF), a protein that induces DNA bending, has been implicated in some instances of IS*1* site recognition (27, 60). While the *nfsA* gene does not have any obvious IHF binding sites, the *nfsB* gene contains one site at bases 640 to 652 that conforms to an IHF binding site consensus sequence, WWWCAWNANNTTA (W is A or T) (28, 31). Notably, all IS elements, five IS*1* and one IS*2*, that integrated near the 3′ end of *nfsB* were inserted within 100 bp of this consensus sequence, and two integration sites were exactly 9 bases on either side. IS*1* is often associated with regional preferences for approximately 100-bp segments of DNA in which they insert throughout (27, 50, 82).

With the exception of IS*186*, all IS elements demonstrated specificity for insertion in the regions proximate to either terminus of *nfsA* and *nfsB*, suggesting that despite the variable target sequence specificity of IS elements, there may be some common determinants in target site selection. Several studies have shown that IS*1* has a preference for insertion into stretches of A+T-rich sequences (44, 50, 82). It has been suggested that IS*1*, like RNA polymerase, may require regions high in A+T for their low helix stability (19, 44, 50), so A+T-rich promoter regions could be expected to be targets for IS*1*. Among the mutants described in the current study, four mutants had IS*1* inserted within the promoter region of *nfsA*, while eight *nfsB* mutants had IS*1* inserted within the first 165 bases of the coding region, which has a high density of homopolymeric runs of adenine and thymine which, according to the wedge model of DNA conformation, could, like IHF (26, 27, 60), promote bending of DNA (30, 32, 38, 74).

ACKNOWLEDGMENTS

We thank Douglas Bryant for providing the original nitrofurazone-resistant mutants used in this study and for his continuing interest in our work. Thanks also go to Suzanne Paterson for her valuable advice on many aspects of this project and for critical reading of the manuscript.

This work was supported by a research grant to I.B.L. from the Natural Science and Engineering Research Council (NSERC) of Canada.

REFERENCES

1. **Altschul, S. F., W. Gish, W. Miller, E. W. Myers, and D. J. Lipman.** 1990. Basic local alignment search tool. J. Mol. Biol. **215:**403–410.
2. **Asnis, R. E.** 1957. The reduction of furacin by cell-free extracts of furacin-resistant and parent-susceptible strains of *Escherichia coli*. Arch. Biochem. Biophys. **66:**208–216.
3. **Bachmann, B. J.** 1972. Pedigrees of some mutant strains of *Escherichia coli* K-12. Bacteriol. Rev. **40:**116–167.
4. **Bauchinger, M., E. Schmid, F. J. Wiebel, and E. Roscher.** 1988. 1,6-Dinitropyrene causes spindle disturbances and chromosomal damage in V79 Chinese hamster cells. Mutat. Res. **208:**213–218.
5. **Beloin, C., S. Ayora, R. Exley, L. Hirschbein, N. Ogasawara, Y. Kasahara, J. C. Alonso, and F. L. Hegarat.** 1997. Characterization of an *lrp*-like (*lrpC*) gene from *Bacillus subtilis*. Mol. Gen. Genet. **256:**63–71.
6. **Birkenbihl, R. P., and W. Vielmetter.** 1989. Complete maps of IS*1*, IS*2*, IS*3*, IS*4*, IS*5*, IS*30* and IS*150* locations in *Escherichia coli* K12. Mol. Gen. Genet. **220:**147–153.
7. **Birkenbihl, R. P., and W. Vielmetter.** 1991. Completion of the IS map in *E. coli*: IS*186* positions on the *E. coli* K-12 chromosome. Mol. Gen. Genet. **226:**318–320.
8. **Blattner, F. R., G. Plunkett III, C. A. Bloch, N. T. Perna, V. Burland, M. Riley, J. Collado-Vides, J. D. Glasner, C. K. Rode, G. F. Mayhew, J. Gregor, N. W. Davis, H. A. Kirkpatrick, M. A. Goeden, D. J. Rose, B. Mau, and Y. Shao.** 1997. The complete genome sequence of *Escherichia coli* K-12. Science **277:**1453–1462.
9. **Boyd, E. F., and D. L. Hartyl.** 1997. Nonrandom location of IS1 elements in the genomes of natural isolates of *Escherichia coli*. Mol. Biol. Evol. **14:**725–732.
10. **Breeze, A. S., and E. E. Obaseiki-Ebor.** 1983. Mutations to nitrofurantoin and nitrofurazone resistance in *Escherichia coli* K12. J. Gen. Microbiol. **129:** 99–103.
11. **Brosius, J.** 1984. Plasmid vectors for the selection of promoters. Gene **27:** 151–160.
12. **Bryant, C., and M. DeLuca.** 1991. Purification and characterization of an oxygen-insensitive NAD(P)H nitroreductase from *Enterobacter cloacae*. J. Biol. Chem. **266:**4119–4125.
13. **Bryant, C., L. Hubbard, and W. D. McElroy.** 1991. Cloning, nucleotide sequence, and expression of the nitroreductase gene from *Enterobacter cloacae*. J. Biol. Chem. **266:**4126–4130.
14. **Bryant, D. W., D. R. McCalla, M. Leeksma, and P. Laneuville.** 1981. Type I nitroreductases of *Escherichia coli*. Can. J. Microbiol. **27:**81–86.
15. **Caspers, P., B. Dalrymple, S. Iida, and W. Arber.** 1984. IS*30*, a new insertion sequence of *Escherichia coli* K12. Mol. Gen. Genet. **196:**68–73.
16. **Chong, P., I. Hui, T. Loo, and S. Gillam.** 1985. Structural analysis of a new GC-specific insertion element IS*186*. FEBS Lett. **192:**47–52.
17. **Coves, J., M. Zeghouf, D. Macherel, B. Guigliarelli, M. Asso, and M. Fontecave.** 1997. Flavin mononucleotide-binding domain of the flavoprotein component of the sulfite reductase from *Escherichia coli*. Biochemistry **36:** 5921–5928.
18. **Craig, N. L.** 1997. Target site selection in transposition. Annu. Rev. Biochem. **66:**437–474.
19. **Das, A., D. Court, M. Gottesman, and S. Adhya.** 1977. Polarity of insertion mutations is caused by Rho-mediated termination of transcription, p. 93–98. *In* A. I. Bukhari, J. A. Shapiro, and S. L. Adhya (ed.) DNA insertion elements, plasmids, and episomes. Cold Spring Harbor Laboratory, Cold Spring Harbor, N.Y.
20. **DeMarini, D. M., M. L. Shelton, and D. A. Bell.** 1996. Mutation spectra of chemical fractions of a complex mixture: role of nitroarenes in the mutagenic specificity of municipal waste incinerator emissions. Mutat. Res. **349:**1–20.
21. **de Serres, F. J., and T. Matsushima.** 1986. Mutagenesis and carcinogenesis by nitropyrenes and cancer chemotherapeutics. Mutat. Res. **164:**3–8.
22. **Djuric, Z., D. W. Potter, R. H. Heflich, and F. A. Beland.** 1986. Aerobic and anaerobic reduction of nitrated pyrenes *in vitro*. Chem.-Biol. Interact. **59:** 309–324.
23. **Drzyzga, O., A. Schmidt, and K.-H. Blotevogel.** 1995. Reduction of nitrated

diphenylamine derivatives under anaerobic conditions. Appl. Environ. Microbiol. **61:**3282–3287.
24. **Eddy, E. P., E. C. McCoy, H. S. Rosenkranz, and R. Mermelstein.** 1986. Dichotomy in the mutagenicity and genotoxicity of nitropyrenes: apparent effect of the number of electrons involved in nitroreduction. Mutat. Res. **161:** 109–111.
25. **Engler, J. A., and M. P. van Bree.** 1981. The nucleotide sequence and protein-coding capability of the transposable element IS5. Gene **14:**155–163.
26. **Galas, D. J., and M. Chandler.** 1989. Bacterial insertion sequences, p. 109–162. *In* D. E. Berg and M. M. Howe (ed.), Mobile DNA. American Society for Microbiology, Washington, D.C.
27. **Gamas, P., M. G. Chandler, P. Prentki, and D. J. Galas.** 1987. *Escherichia coli* integration host factor binds specifically to the ends of the insertion sequence IS*1* and to its major insertion hot-spot in pBR322. J. Mol. Biol. **195:**261–272.
28. **Goodrich, J. A., M. L. Schwartz, and W. R. McClure.** 1990. Searching for and predicting the activity of sites for DNA binding proteins: compilation and analysis of the binding sites for *Escherichia coli* integration host factor (IHF). Nucleic Acids Res. **18:**4993–5000.
29. **Goodwin, A., D. Kersulyte, G. Sisson, S. J. O. Veldhuyzen van Zanten, D. E. Berg, and P. S. Hoffman.** 1998. Metronidazole resistance in Helicobacter pylori is due to null mutations in a gene (rdxA) that encodes an oxygen-insensitive NADPH nitroreductase. Mol. Microbiol. **28:**383–393.
30. **Hagerman, P. J.** 1990. Sequence-directed curvature of DNA. Annu. Rev. Biochem. **59:**755–781.
31. **Hales, L. M., R. I. Gumport, and J. F. Gardner.** 1994. Determining the DNA sequence elements required for binding integration host factor to two different target sites. J. Bacteriol. **176:**2999–3006.
32. **Harrington, R. E.** 1992. DNA curving and bending in protein-DNA recognition. Mol. Microbiol. **6:**2549–2555.
33. **Hecht, H. J., H. Erdmann, H. J. Park, M. Sprinzl, and R. D. Schmid.** 1995. Crystal structure of NADH oxidase from *Thermus thermophilus*. Nat. Struct. Biol. **2:**1109–1114.
34. **Higgins, D., and P. M. Sharp.** 1989. Fast and sensitive multiple sequence alignments on a microcomputer. CABIOS **5:**151–153.
35. **Hodgson, A. V., and H. W. Strobel.** 1996. Characterization of the FAD binding domain of cytochrome P450 reductase. Arch. Biochem. Biophys. **325:**99–106.
36. **Holmes, D. S., and M. Quigley.** 1981. A rapid boiling method for the preparation of bacterial plasmids. Anal. Biochem. **114:**193–197.
37. **King, C. M.** 1988. Metabolism and biological effects of nitropyrene and related compounds. Research Report no. 16. Health Effects Institute, Cambridge, Mass.
38. **Koo, H.-S., H.-M. Wu, and D. M. Crothers.** 1986. DNA bending at adenine-thymine tracts. Nature **320:**501–506.
39. **Kothary, R. K., D. Johnes, and E. P. Candido.** 1985. IS*186*: an *Escherichia coli* insertion element isolated from a cDNA library. J. Bacteriol. **164:**957–959.
40. **Li, R., M. A. Bianchet, P. Talalay, and L. M. Amzel.** 1995. The three-dimensional structure of NAD(P)H:quinone reductase, a flavoprotein involved in cancer chemoprotection and chemotherapy: mechanism of the two-electron reduction. Proc. Natl. Acad. Sci. USA **92:**8846–8850.
41. **Lu, C., and D. R. McCalla.** 1978. Action of some nitrofuran derivatives on glucose metabolism, ATP levels and macromolecule synthesis in *Escherichia coli*. Can. J. Microbiol. **24:**650–657.
42. **Mason, J. R., and R. Cammack.** 1992. The electron-transport proteins of hydroxylating bacterial dioxygenases. Annu. Rev. Microbiol. **46:**277–305.
43. **Mason, R. P., and J. L. Holtzman.** 1975. The role of catalytic superoxide formation in the oxygen inhibition of nitroreductase. Biochem. Biophys. Res. Commun. **67:**1267–1274.
44. **Matsutani, S.** 1997. Genetic analyses of the interactions of the IS1-encoded proteins with the left end of IS1 and its insertion hotspot. J. Mol. Biol. **267:** 548–560.
45. **McCalla, D. R., A. Reuvers, and C. Kaiser.** 1970. Mode of action of nitrofurazone. J. Bacteriol. **104:**1126–1134.
46. **McCalla, D. R., P. Olive, Y. Tu, and M. L. Fan.** 1975. Nitrofurazone-reducing enzymes in *E. coli* and their role in drug activation *in vivo*. Can. J. Microbiol. **21:**1485–1491.
47. **McCalla, D. R., D. Voutsinos and P. L. Olive.** 1975. Mutagen screening with bacteria: niridazole and nitrofurans. Mutat. Res. **31:**31–37.
48. **McCalla, D. R., C. Kaiser, and M. H. L. Green.** 1978. Genetics of nitrofurazone resistance in *Escherichia coli*. J. Bacteriol. **133:**10–16.
49. **McCalla, D. R.** 1979. Nitrofurans, p. 176–213. *In* F. E. Hahn (ed.), Mechanism of action of antibacterial agents. Springer-Verlag, Berlin, Germany.
50. **Meyer, J., S. Iida, and W. Arber.** 1980. Does the insertion element IS*1* transpose preferentially into A+T-rich DNA segments? Mol. Gen. Genet. **178:**471–473.
51. **Michael, N. P., J. K. Brehm, G. M. Anlezark, and N. P. Minton.** 1994. Physical characterization of the *Escherichia coli B* gene encoding nitroreductase and its over-expression in *Escherichia coli* K12. FEMS Microbiol. Lett. **124:**195–202.
52. **Möller, L., I. Lax, and L. C. Eriksson.** 1993. Nitrated polycyclic aromatic hydrocarbons: a risk assessment for the urban citizen. Environ. Health Perspect. Suppl. **101:**309–315.
53. **Naas, T., M. Blot, W. M. Fitch, and W. Arber.** 1994. Insertion sequence-related genetic variation in resting *Escherichia coli* K-12. Genetics **136:**721–730.
54. **Narayanasami, R., P. M. Horowitz, and B. S. S. Masters.** 1995. Flavin-binding and protein structural integrity studies on NADPH-cytochrome P450 reductase are consistent with the presence of distinct domains. Arch. Biochem. Biophys. **316:**267–274.
55. **Niedle, E. L., C. Harnett, L. N. Ornston, A. Bairoch, M. Rekik, and S. Harayama.** 1991. Nucleotide sequences of the *Acinetobacter calcoaceticus benABC* genes for benzoate 1,2-dioxygenase reveal evolutionary relationships among multicomponent oxygenases. J. Bacteriol. **173:**5385–5395.
56. **Niviere, V., F. Fieschi, J.-L. Decout, and M. Fontecave.** 1996. Is the NAD(P)H:flavin oxidoreductase from *Escherichia coli* a member of the ferredoxin-NADP$^+$ reductase family? J. Biol. Chem. **271:**16656–16661.
57. **Ohtsubo, E., and Y. Sekine.** 1996. Bacterial insertion sequences. Curr. Top. Microbiol. Immunol. **204:**1–26.
58. **Ostrowski, J., M. J. Barber, D. C. Rueger, B. E. Miller, L. M. Siegel, and N. M. Kredich.** 1989. Characterization of the flavoprotein moieties of NADPH-sulfite reductase from *Salmonella typhimurium* and *Escherichia coli*. J. Biol. Chem. **264:**15796–15808.
59. **Peterson, F. J., R. P. Mason, J. Hovsepian, and J. L. Holtzman.** 1979. Oxygen-sensitive and -insensitive nitroreduction by *Escherichia coli* and rat hepatic microsomes. J. Biol. Chem. **254:**4009–4014.
60. **Prentki, P., M. Chandler, and D. J. Galas.** 1987. *Escherichia coli* integration host factor bends the DNA at the ends of IS*1* and in an insertion hotspot with multiple IHF binding sites. EMBO J. **6:**2479–2487.
61. **Rodriguez, R. L., and R. C. Tait.** 1983. Recombinant DNA techniques: an introduction, p. 37–46, 187–192. Benjamin/Cummings Publishing Company, Inc., Menlo Park, Calif.
62. **Rosenkranz, H. S., E. C. McCoy, D. R. Sanders, M. Butler, D. K. Kiriazides, and R. Mermelstein.** 1980. Nitropyrenes: isolation, identification, and reduction of mutagenic impurities in carbon black and toners. Science **209:**1039–1042.
63. **Salmeen, I., A. M. Durisin, T. J. Prater, T. Riley, and D. Schuetzle.** 1982. Contribution of 1-nitropyrene to direct-acting Ames assay mutagenicities of diesel particulate extracts. Mutat. Res. **104:**17–23.
64. **Sastry, S. S., and R. Jayaraman.** 1984. Nitrofurantoin-resistant mutants of *Escherichia coli*: isolation and mapping. Mol. Gen. Genet. **196:**379–380.
65. **Sengstag, C. S. Iida, R. Hiestand-Nauer, and W. Arber.** 1986. Terminal inverted repeats of prokaryotic transposable element IS*186* which can generate duplications of variable length at an identical target sequence. Gene **49:**153–156.
66. **Shaw, W. V.** 1975. Chloramphenicol acetyltransferase from chloramphenicol-resistant bacteria. Methods Enzymol. **43:**737–755.
67. **Spain, J. C.** 1995. Biodegradation of nitroaromatic compounds. Annu. Rev. Microbiol. **49:**523–555.
68. **Szybalski, W., and V. Bryson.** 1952. Genetic studies on microbial cross resistance to toxic agents. J. Bacteriol. **64:**489–499.
69. **Tanner, J. J., B. Lei, S.-C. Tu, and K. L. Krause.** 1996. Flavin reductase P: structure of a dimeric enzyme that reduces flavin. Biochemistry **35:**13531–13539.
70. **Tazima, Y., T. Kada, and A. Murakami.** 1975. Mutagenicity of nitrofuran derivatives, including furylfuramide, a food preservative. Mutat. Res. **32:**55–80.
71. **Tokiwa, H., and Y. Ohnishi.** 1986. Mutagenicity and carcinogenicity of nitroarenes and their sources in the environment. Crit. Rev. Toxicol. **17:**23–60.
72. **Tomb, J.-F., O. White, A. R. Kerlavage, R. A. Clayton, G. G. Sutton, R. D. Fleischmann, K. A. Ketchum, H. P. Klenk, S. Gill, B. A. Dougherty, K. Nelson, J. Quackenbush, L. Zhou, E. F. Kirkness, S. Peterson, B. Loftus, D. Richardson, R. Dodson, H. G. Khalak, A. Glodek, K. McKenney, L. M. Fitzegerald, N. Lee, M. D. Adams, E. K. Hickey, D. E. Berg, J. D. Gocayne, T. R. Utterback, J. D. Peterson, J. M. Kelley, M. D. Cotton, J. M. Weidman, C. Fujii, C. Bowman, L. Watthey, E. Wallin, W. S. Hayes, M. Borodovsky, P. D. Karp, H. O. Smith, C. M. Fraser, and J. C. Venter.** 1997. The complete genome sequence of the gastric pathogen *Helicobacter pylori*. Nature **388:** 539–547.
73. **Tu, Y., and D. R. McCalla.** 1975. Effect of activated nitrofurans on DNA. Biochim. Biophys. Acta **402:**142–149.
74. **Ulanovsky, L. E., and E. N. Trifonov.** 1987. Estimation of wedge components in curved DNA. Nature **326:**720–722.
75. **Umeda, M., and E. Ohtsubo.** 1990. Mapping of insertion element IS*30* in the *Escherichia coli* K12 chromosome. Mol. Gen. Genet. **222:**317–322.
76. **Vieira, J., and J. Messing.** 1982. The pUC plasmids, an M13mp7-derived system for insertion mutagenesis and sequencing with synthetic universal primers. Gene **34:**87–93.
77. **Wasserfallen, A., K. Huber, and T. Leisinger.** 1995. Purification and structural characterization of a flavoprotein induced by iron limitation in *Methanobacterium thermoautotrophicum* Marburg. J. Bacteriol. **177:**2436–2441.
78. **Watanabe, M., M. Ishidate, Jr., and T. Nohmi.** 1990. Nucleotide sequence

of *Salmonella typhimurium* nitroreductase gene. Nucleic Acids Res. **18:**1059.
79. **Zenno, S., H. Koike, A. N. Kumar, R. Jayaraman, M. Tanokura, and K. Saigo.** 1996. Biochemical characterization of NfsA, the *Escherichia coli* major nitroreductase exhibiting a high amino acid sequence homology to Frp, a *Vibrio harveyi* flavin oxidoreductase. J. Bacteriol. **178:**4508–4514.
80. **Zenno, S., H. Koike, M. Tanokura, and K. Saigo.** 1996. Conversion of NfsB, a minor *Escherichia coli* nitroreductase, to a flavin reductase similar in biochemical properties to FRase I, the major flavin reductase in *Vibrio fischeri*, by a single amino acid substitution. J. Bacteriol. **178:**4731–4733.
81. **Zenno, S., K. Saigo, H. Kanoh, and S. Inouye.** 1994. Identification of the gene encoding the major NAD(P)H-flavin oxidoreductase of the bioluminescent bacterium *Vibrio fischeri* ATCC 7744. J. Bacteriol. **176:**3536–3543.
82. **Zerbib, D., P. Gamas, M. Chandler, P. Prentki, S. Bass, and D. Galas.** 1985. Specificity of insertion of IS*1*. J. Mol. Biol. **185:**517–524.